CEA-CONF--11464

FR9303735

Title: Modelling of cladding creep collapse

CEA-CONF-11469
FR9303735

ABSTRACT

The effects of the initial ovality and pressure level on the collapse time of Zircaloy-4 tubing subjected to uniform external pressure were examined experimentally and analytically. Experiments were performed on end closed tubes with two metallurgical states : stress relieved and recrystallized. Numerical simulations were accomplished with a specific computer program based on an analytical approach and the calculated results were compared with the experimental ones. As a comparison, the finite element method is also partially examined in this analysis. Numerical collapse times are in good agreement with regard to experimental results in the case of stress relieved structure. They seem to be too conservative in the case of a recrystallized metallurgical state and the use of the anisotropic option ameliorates numerical results. Sensibility of numerical solutions to the formulation of primary creep laws are presented.

1 INTRODUCTION

The LWR's fuel rods are designed to preclude creep collapse of an eventual unsupported part of the cladding. Long term flattening of the cladding could result from the combined action of the design (clad thickness, initial ovality,...) and of the irradiation conditions (fast neutron flux, temperature, pressure) leading to the instability threshold of the cladding due to creep deformation.

In the framework of the development of new cladding materials, CEA and FRAMATOME have undertaken a joint R&D program. On the one hand, to get a better understanding of the mechanisms of long time creep phenomena, by achieving out-of-pile tests to study the influence of initial ovality and creep behaviour of the material on clad flattening. On the other hand, to validate a numerical approach of the cladding behaviour with regard to creep collapse phenomena and to define the sensibility to various parameters (anisotropy, primary creep, mechanical modelling).

Flattening creep time measurements were conducted first on reference test tubes with different initial ovalities. Zircaloy-4 tubes were exposed to chosen external pressure, at a test temperature of 400°C. These creep collapse tests enabled us to determine curves giving the circumferential flattening time of a tube as a function of the initial ovality for various values of the external pressure, yielding the different mechanical behaviours relevant to the stress relieved and recrystallized states.

Numerical calculations were performed with a specific cladding creep collapse code and a finite element code, in order to compare numerical and experimental results. The specific code is developed from analytical equations and can handle any combination of either strain hardening or time hardening forms, isotropic or anisotropic effects and the Mises flow rule or the Tresca flow rule.

2 EXPERIMENTAL PROGRAM

2.1 Test apparatus

The test apparatus is shown in figure 1. The specimen was placed on a support sustained by a stainless steel rod into a pressured vessel heated by an electrical resistance furnace. The test apparatus can be operated at a pressure of up to 30 MPa and the temperature was adjusted to a value of 400 °C. The isothermal zone of the furnace is about 100 mm in length and the regulated temperature is controlled to within ± 2 °C by five thermocouples. External pressure on the specimen is supplied by argon gas and controlled to within ± 0.2 MPa. The creep collapse time was detected by the sudden decrease of pressure which was observed by a pressure gauge.

2.2 Test tubes

The test tubes were hermetically closed by two electron beam welded plugs at the extremities. Their dimensions were 9.5 mm in outer diameter, 0.584 mm in wall thickness and 140 mm in length. Their ovality was defined by $(\phi_{max} - \phi_{min})$ where ϕ_{max} and ϕ_{min} are the maximum and the minimum outer diameters, respectively. Their natural and initial ovalizations were slight and observed locally. More important initial ovalities were needed in the experimental program, especially for the values which vary between 0.01 mm and 0.15 mm. In order to obtain a uniform and quasi-elliptical cross section along their length, the specimens were deformed by applying a diametral compression between two parallel flat plates set up on an hydroelectric machine.

2.3 Experimental results

Experiments were performed for four external pressures in the range from $p = 0.15\, p_{crit}$ to $p = 0.30\, p_{crit}$, where p_{crit} denotes the elastic buckling critical pressure for a long perfect thin tube under external pressure [1].

As an example, the experimental collapse time as a function of initial ovality, in the case of the external pressure of $p = 0.25\, p_{crit}$, is shown in figure 2, for the two metallurgical state tubes. This result points out the effect of recrystallization on thin-walled tubing : the recrystallized material seems to have a higher resistance to creep ovalization than the stress relieved one for external pressurization.

3 NUMERICAL SIMULATIONS

3.1 Creep constitutive equations

Two kinds of formulation are chosen for the numerical analysis. Both of them link the creep tangential strain ε_θ to the tangential stress σ_θ, depending on time t and temperature T.

Type I formulation :

$$\varepsilon_\theta = A\, \sigma_\theta^n\, t^m\, e^{(-B/T)} \quad (2)$$

Type II formulation :

$$\varepsilon_\theta = B_1 t + B_2 (1 - e^{-B_3 t}) \quad (3)$$

where

n, m, A, B : numerical coefficients,

B_1, B_2, B_3 : functions of σ, T .

Figure 3 presents the graphs of curves from equations (2) and (3), obtained by fit on experimental points (dashed lines for the formulation I and solid lines for the formulation II). We note that only the second formulation can correctly describe the secondary stage of creep and that, in the range of primary creep, the slops of these two curves, especially at small values of time where experimental points are not available, are significantly different.

In order to study the sensibility of this difference, the third law derived from the second one is used.

Type III formulation :

$$\varepsilon_\theta = B_1 t + (1-\alpha) B_2 (1-e^{-B_3 t}) + \alpha B_2 (1-e^{-B_4 t}) \qquad (4)$$

where B_4 is a function of B_3. We can note that the formulations II and III have the same asymptotic line and are identical when $\alpha = 0$. This third formulation with the parameter α provides, at the beginning of primary creep, a bundle of curves between the two curves relating to the formulations I and II (fig. 3).

3.2 Analytical code

The analytical method is the same as the one presented by W.K. WILSON [2] and P.LEMOINE [3]. It is applied to thin shell structures which are supposed to be long enough to neglect the end effects. Initial out-of-roundness and deflection are not functions of the axial co-ordinate. The total axial strain is a function of time and not a function of the radial or tangential co-ordinates. It is a numerical step by step method in which time is divided up into a large number of small time increments. The conditions of equilibrium and compatibility must be satisfied at all steps. The combination of equilibrium equations, constitutive equations and strain expressions leads to the following type of differential equation :

$$\frac{d^2 w(\theta)}{d\theta^2} + m^2 w(\theta) = F(\theta) \qquad (5)$$

The solution of (5) is obtained by representing $F(\theta)$ as a Fourier series and is achieved in two distinct periods : an explicit solving of the elastic problem for the first step and a step by step solving of the creep problem for the others. The analytical procedure is written in FORTRAN 77 and the calculations are performed on a PC 486.

3.3 Finite element code

As a comparison, calculations were also partially performed by a general finite element code CASTEM [4]. The generalized plane strain is selected and the two-node thin shell element in large displacements with nine integration points is adopted. The update Lagrangian formulation is used and the change of direction of the external pressure caused by the deformation of the outer surface is taken into account.

As in the analytical code, stress-strain and deflection are elastic in the first step. The creep calculations start from the second step and the collapse time is established when the relative ovality $(\phi_{max} - \phi_{min}) / \phi_m$ reaches 100 %; ϕ_m denotes the mean diameter.

3.3 Comparison of results and discussion

Figure 4 shows the collapse time curves obtained in the case of stress relieved state by the analytical and finite element codes, for various initial ovalities and under the pressure of $p = 0.20\, p_{crit}$. Experimental results are also plotted on the same figure for comparison. The calculations were performed with an isotropic Von Mises flow rule. The significant influence on calculated collapse caused by using the time hardening form as compared with the strain hardening form, as well as the influence due to the two types of formulation selected for numerical analysis are evidenced on figure 4. It was found that only the first formulation of creep law and the strain hardening form led to conservative results.

The effect of primary creep law formulation can be seen here, in the case of strain hardening form, by the difference between the curves SH1 (formulation I) and SH2 (formulation II). This difference could be reduced by raising the value of α, in the formulation III, from 0 to 0.28 as shown in the table 1. The variation of α brought the curve SH2 near to SH1.

TABLE 1. Collapse time as a function of α, calculated with formulation III, for 0.120mm in initial ovality and under the pressure of $p = 0.20\, p_{crit}$.

α	0	0.15	0.20	0.28
Time (hours)	221	170	138	65

First formulation and strain hardening form were adopted for numerical simulations in the case of stress relieved material. The comparison of collapse times, for various pressures and for various initial ovalities, between the experiments and the analytical calculations, is presented in figure 5. It is shown that the predictions of the creep buckling time of the tube under external pressure by the analytical simplified method are in good agreement with the experimental results.

The calculations are also made for the recrystallized tubing, with the formulation I in a strain hardening form, which is the more suitable. Otherwise, it doesn't give good results. Recrystallization treatment modifies the anisotropy; so, a calculation is made by introducing anisotropic coefficients, evaluated from closed-end biaxial creep tests on Zircaloy. The modified Von Mises criterion for an anisotropic material and the generalized stress is used in the analytical method. The anisotropic option ameliorates numerical simulations as shown in table 2.

TABLE 2. Anisotropic effect on collapse time (hours), calculated in the case of $p = 0.20\, p_{crit}$ and with formulation I.

Initial ovality (microns)	30	50	120
Isotropic case	623	431	176
Anisotropic case	1001	708	304
Experiments	1668	1378	383

4 CONCLUSION

Creep buckling tests and analysis of thin-walled tubes subjected to external pressures were performed. Creep buckling phenomenon is, as well known, very sensitive to the smallest variation of initial parameters. It is highly satisfactory that the experimental results fall within the limits determined by a simplified analytical calculation. This analytical simulation is interesting, especially when it is necessary to perform a large number of calculations to study the effects of the geometrical characteristics and material behaviour of the tube on the collapse time, because of the easiness of the numerical model. The mesh of the tube is simply limited to initial ovality, radius and thickness.

References

[1] S. Timoshenko, "Theory of Elastic Stability "McGraw-Hill, New York,1961.
[2] W.K. Wilson, "A method of analysis for the creep-buckling of tubes under external pressure", WAPD-TM-956, 1970.
[3] P. Lemoine, J.M. Frenkel, M. Weisz, "Validation of in-pile creep collapse analyses of

Zircaloy cladding by direct experiments ", Vol.C., 4th S.M.I.R.T.,1977.
[4] A. Combescure, INCA Manuel- CASTEM System, CEA, 1985.

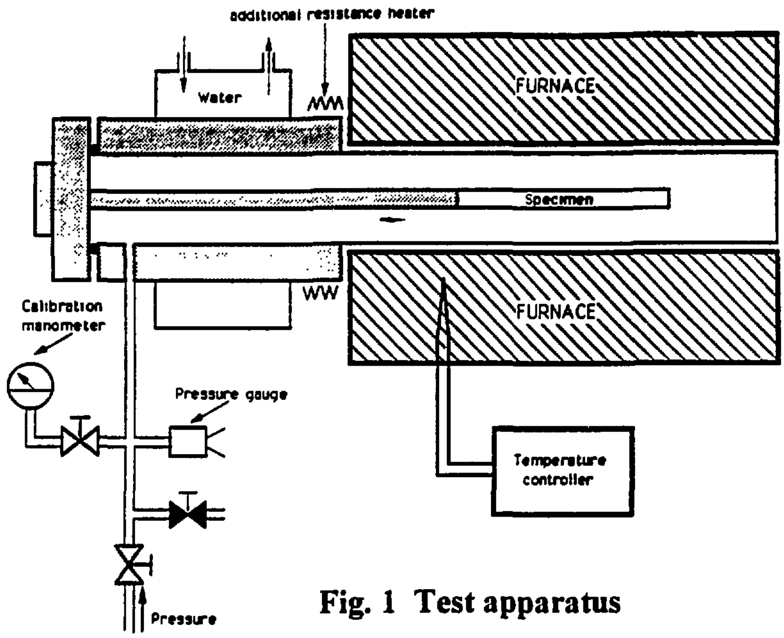

Fig. 1 Test apparatus

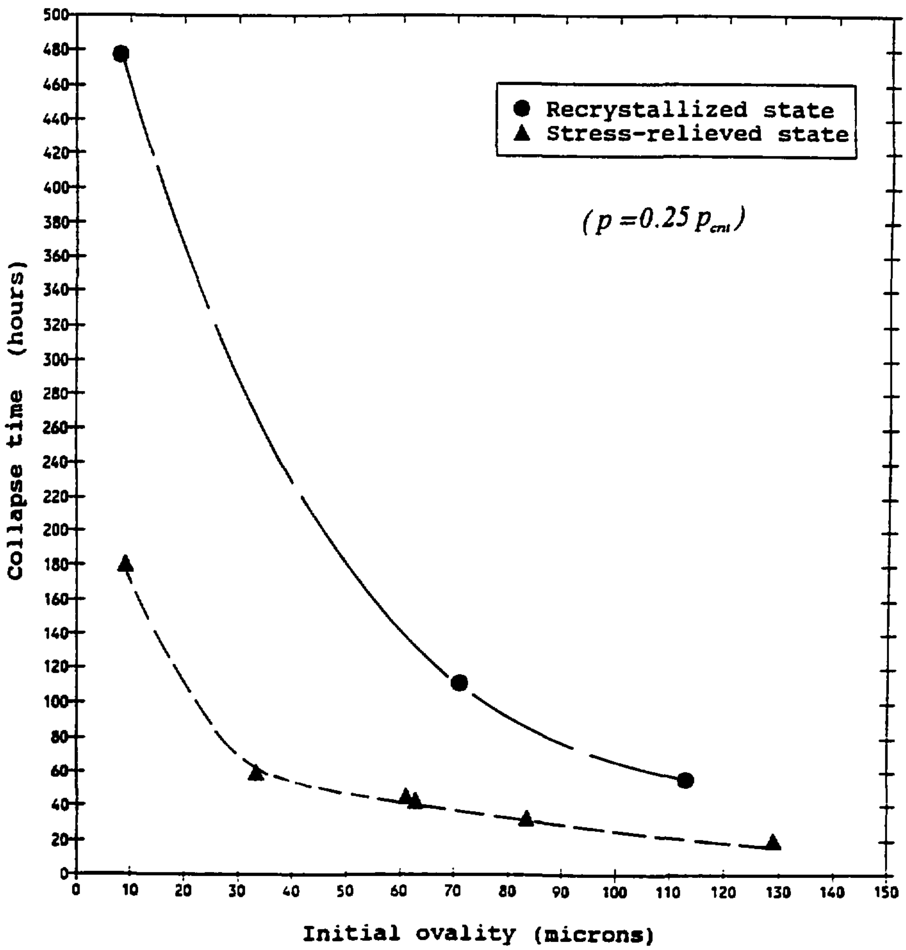

Fig. 2 Experimental collapse time as a function of initial ovality, under an external pressure of 0.25 p_{crit}

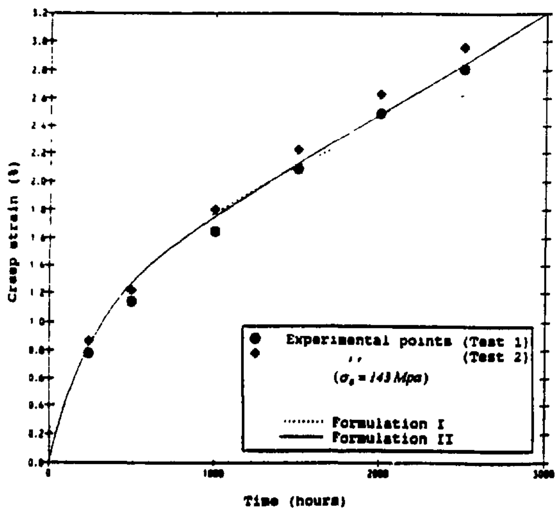

Fig. 3 Creep law forms used in the numerical analysis

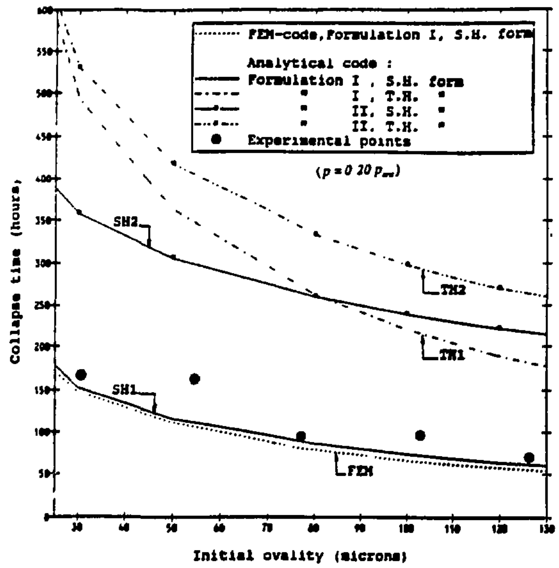

Fig. 4 Collapse time as a function of initial ovality, under a pressure of 0.20 p_{crit}

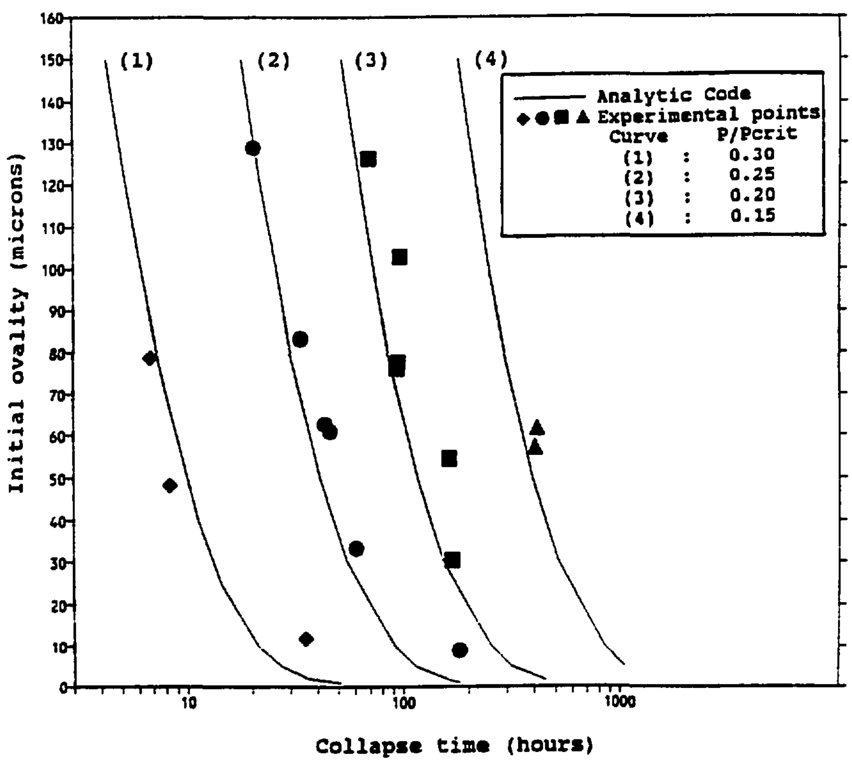

Fig. 5. Calculated collapse time curves obtained by the analytical code, in comparison with the experimental values, for various pressures and various initial ovalities, in the case of stress relieved material